

### [Synthesis, structure, and properties of \$\text{Ba}\_9\text{Co}\_3\text{Se}\_{15}\$ with one-dimensional spin chains](#)

Lei Duan(段磊), Xian-Cheng Wang(望贤成), Jun Zhang(张俊), Jian-Fa Zhao(赵建发), Li-Peng Cao(曹立朋), Wen-Min Li(李文敏), Run-Ze Yu(于润泽), Zheng Deng(邓正), Chang-Qing Jin(靳常青)

**Citation:** Chin. Phys. B . 2020, 29(3): 036102 . doi: 10.1088/1674-1056/ab69ea

Journal homepage: <http://cpb.iphy.ac.cn>; <http://iopscience.iop.org/cpb>

What follows is a list of articles you may be interested in

---

### [Crystal structure and magnetic properties of disordered alloy \$\text{ErGa}\_{3-x}\text{Mn}\_x\$](#)

Cong Wang(王聪), Yong-Quan Guo(郭永权), Shuo-Wang Yang(杨硕望)

Chin. Phys. B . 2019, 28(8): 086101 . doi: 10.1088/1674-1056/28/8/086101

### [Isostructural phase transition-induced bulk modulus multiplication in dopant-stabilized \$\text{ZrO}\_2\$ solid solution](#)

Min Wang(王敏), Wen-Shu Shen(沈文舒), Xiao-Dong Li(李晓东), Yan-Chun Li(李延春), Guo-Zhao Zhang(张国召), Cai-Long Liu(刘才龙), Lin Zhao(赵琳), Shu-Peng Lv(吕舒鹏), Chun-Xiao Gao(高春晓), Yong-Hao Han(韩永昊)

Chin. Phys. B . 2019, 28(7): 076109 . doi: 10.1088/1674-1056/28/7/076109

### [Recent progress on magnetic-field studies on quantum-spin-liquid candidates](#)

Zhen Ma(马祯), Kejing Ran(冉柯静), Jinghui Wang(王靖琿), Song Bao(鲍嵩), Zhengwei Cai(蔡正蔚), Shichao Li(李世超), Jinsheng Wen(温锦生)

Chin. Phys. B . 2018, 27(10): 106101 . doi: 10.1088/1674-1056/27/10/106101

### [Local microstructural analysis for \$\text{Y}\_2\text{O}\_3/\text{Eu}^{3+}/\text{Mg}^{2+}\$ nanorods by Raman and photoluminescence spectra under high pressure](#)

Jin-Hua Wang(王金华), Ze-Peng Li(李泽朋), Bo Liu(刘波), Bing-Bing Liu(刘冰冰)

Chin. Phys. B . 2017, 26(2): 026101 . doi: 10.1088/1674-1056/26/2/026101

### [High-pressure structure and elastic properties of tantalum single crystal: First principles investigation](#)

Jian-Bing Gu(顾建兵), Chen-Ju Wang(王臣菊), Wang-Xi Zhang(张旺玺), Bin Sun(孙斌), Guo-Qun Liu(刘国群), Dan-Dan Liu(刘丹丹), Xiang-Dong Yang(杨向东)

Chin. Phys. B . 2016, 25(12): 126103 . doi: 10.1088/1674-1056/25/12/126103

---

# Synthesis, structure, and properties of $\text{Ba}_9\text{Co}_3\text{Se}_{15}$ with one-dimensional spin chains\*

Lei Duan(段磊)<sup>1,2</sup>, Xian-Cheng Wang(望贤成)<sup>1,†</sup>, Jun Zhang(张俊)<sup>1,2</sup>, Jian-Fa Zhao(赵建发)<sup>1,2</sup>, Li-Peng Cao(曹立朋)<sup>1,2</sup>, Wen-Min Li(李文敏)<sup>1,2</sup>, Run-Ze Yu(于润泽)<sup>1</sup>, Zheng Deng(邓正)<sup>1</sup>, and Chang-Qing Jin(靳常青)<sup>1,2,3,‡</sup>

<sup>1</sup>Institute of Physics, Chinese Academy of Sciences, Beijing 100190, China

<sup>2</sup>School of Physics, University of Chinese Academy of Sciences, Beijing 100190, China

<sup>3</sup>Materials Research Laboratory at Songshan Lake, Dongguan 523808, China

(Received 26 November 2019; revised manuscript received 6 January 2020; accepted manuscript online 10 January 2020)

A new compound with one-dimensional spin chains,  $\text{Ba}_9\text{Co}_3\text{Se}_{15}$ , was synthesized under high pressure and high temperature conditions and systematically characterized via structural, transport and magnetic measurements.  $\text{Ba}_9\text{Co}_3\text{Se}_{15}$  crystallizes in a hexagonal structure with the space group  $P-6c2$  (No. 188) and lattice constants of  $a = b = 9.6765 \text{ \AA}$  and  $c = 18.9562 \text{ \AA}$ . The structure consists of trimeric face-sharing octahedral  $\text{CoSe}_6$  chains, which are arranged in a triangular lattice in the  $ab$ -plane and separated by Ba atoms. The distance of the nearest neighbor of  $\text{CoSe}_6$  chains is very large, given by the lattice constant  $a = 9.6765 \text{ \AA}$ . The Weiss temperature  $T_\theta$  associated with the intra-chain coupling strength is about  $-346 \text{ K}$ . However, no long-range magnetic order but a spin glass transition at  $\sim 3 \text{ K}$  has been observed. Our results indicate that the spin glass behavior in  $\text{Ba}_9\text{Co}_3\text{Se}_{15}$  mainly arises from the magnetic frustration due to the geometrically frustrated triangular lattice.

**Keywords:** one-dimensional chain, spin glass, high-pressure

**PACS:** 61.05.cp, 61.50.-f, 61.66.Fn, 61.82.Fk

**DOI:** 10.1088/1674-1056/ab69ea

## 1. Introduction

Quasi-one-dimensional (1D) system exhibits many exotic physical phenomena due to the reduction of dimensions. It is well known that for an ideal 1D spin chain, the thermal and quantum fluctuations prevent the formation of a long-range order at finite temperature.<sup>[1]</sup> However, for a system with quasi 1D spin chains, the inter-chain spin interaction usually results in the long-range magnetic transition although it generally is very weak. It is especially interesting when these spin chains are arranged in a triangular lattice, which would induce geometric magnetic frustration and give rise to rich ground states. The prominent example is the composition  $ABX_3$  ( $A$  is alkali metal,  $B$  is 3d transition metal,  $X$  is halogen atom), where the infinite face-sharing  $BX_6$  octahedral chains are triangularly arranged in the  $ab$ -plane.<sup>[2]</sup> For these  $ABX_3$  compounds, the intra-chain exchange interaction is typically two to three orders of magnitude larger than the inter-chain coupling, presenting strongly 1D magnetic properties. Complex spin arrangements in the  $ABX_3$  compounds have been reported due to the frustrated antiferromagnetic interaction.<sup>[3–10]</sup> To partially relieve the frustration effect, the spins on the three sublattices usually form  $120^\circ$  angles with the nearest neighbors on the other sublattices for Heisenberg triangular antiferromagnets. While for Ising triangular antiferromagnets ( $\text{CsCoCl}_3$ <sup>[3,5]</sup> and

$\text{CsCoBr}_3$ <sup>[10]</sup>), the frustration effect becomes more acute and leads to either partial ordered state or fully ordered ferromagnetic state in the triangular plane.

Besides the triangular antiferromagnet of halogenides, the isostructural chalcogenide  $\text{BaVS}_3$  with octahedral  $\text{VS}_6$  chains has been extensively studied.<sup>[11–14]</sup> A metal–insulator transition at  $69 \text{ K}$  driven by Peierls instability was observed and in sequence an incommensurate antiferromagnetic transition occurred at  $\sim 31 \text{ K}$ .<sup>[11]</sup> When the S atoms in  $\text{BaVS}_3$  were replaced with Se,  $\text{BaVSe}_3$  was reported to be a ferromagnetic metal.<sup>[15]</sup> Recently, in order to further enhance the distance of the nearest neighbor chains to enhance the 1D nature,  $\text{Ba}_9\text{V}_3\text{Se}_{15}$  has been synthesized, which undergoes a ferrimagnetic transition at  $2.5 \text{ K}$  and presents 1D ferromagnetic chains properties, i.e.,  $T^{1/2}$  magnetic specific heat above the ordered temperature.<sup>[16]</sup>

Here, we report a new compound  $\text{Ba}_9\text{Co}_3\text{Se}_{15}$ , which is isostructural with  $\text{Ba}_9\text{V}_3\text{Se}_{15}$ , consisting of trimerized face-sharing octahedral  $\text{CoSe}_6$  chains. Although the Weiss temperature associated with the intra-chain coupling strength is about  $-346 \text{ K}$ , no long-range order but spin glass ground state is observed with the frozen temperature  $T_f \sim 3 \text{ K}$ , which is speculated to be caused by the magnetic frustration due to the geometrically frustrated triangular lattice in  $\text{Ba}_9\text{Co}_3\text{Se}_{15}$ .

\*Project supported by the National Key R&D Program of China and the National Natural Science Foundation of China (Grant Nos. 2018YFA0305700, 2017YFA0302900, 11974410, and 11534016).

†Corresponding author. E-mail: wangxiancheng@aphy.iphy.ac.cn

‡Corresponding author. E-mail: jin@iphy.ac.cn

## 2. Experimental methods

The synthesis of  $\text{Ba}_9\text{Co}_3\text{Se}_{15}$  was carried out under high pressure and high temperature conditions using a DS  $6 \times 800$  T cubic anvil high-pressure apparatus. The fine powders of Co (Alfa, 99.99% pure) and Se (Alfa, 99.999% pure), and lumps of Ba (Alfa, immersed in oil, > 99.2% pure) were used as the starting materials. The precursor BaSe was prepared through the reaction of the Ba blocks and Se powder in an alumina crucible sealed in an evacuated quartz tube at 700 °C for 24 h. The mixture of BaSe, Co, and Se was homogeneously mixed at the molar ratio of 3 : 1 : 2, pressed into a pellet with a diameter of 6 mm, and then subjected to high-pressure synthesis under 5.5 GPa and 1000 °C for 40 min. The pressure was released after the temperature was quenched to room temperature, after which the black polycrystalline sample of  $\text{Ba}_9\text{Co}_3\text{Se}_{15}$  was obtained.

The x-ray diffraction (XRD) was conducted on a Rigaku Ultima VI (3 kW) diffractometer using Cu  $K_\alpha$  radiation generated at 40 kV and 40 mA. The Rietveld refinements on the diffraction patterns were performed using the GSAS software package.<sup>[17]</sup> The chemical composition of the  $\text{Ba}_9\text{Co}_3\text{Se}_{15}$  sample was determined through energy dispersive x-ray spectroscopy (EDX). The electrical resistivity  $\rho(T)$  and ac magnetic susceptibility measurements were carried out in a physical property measuring system (PPMS), and the dc magnetic susceptibility was measured by a superconducting quantum interference device (SQUID-VSM, Quantum Design).

## 3. Results and discussion

Polycrystalline sample of  $\text{Ba}_9\text{Co}_3\text{Se}_{15}$  was synthesized under high-pressure and high-temperature conditions. The chemical composition of  $\text{Ba}_9\text{Co}_3\text{Se}_{15}$  was determined by EDX as shown in Fig. 1(a). The inset shows the shining surface of the sample with the grain size about 40  $\mu\text{m}$ . EDX measurement was performed at several different areas on the surfaces, and the average atomic ratio of Ba : Co : Se is about 3.02 : 0.95 : 5.01, which is very close to the stoichiometric ratio of  $\text{Ba}_9\text{Co}_3\text{Se}_{15}$ .

The powder XRD pattern measured at room temperature is shown in Fig. 1(b). All the peaks can be indexed by a hexagonal structure with the lattice parameters of  $a = b = 9.6765 \text{ \AA}$  and  $c = 18.9562 \text{ \AA}$ . The crystal structure of recently discovered compound  $\text{Ba}_9\text{V}_3\text{Se}_{15}$  with a hexagonal structure and the space group  $P-6c2$  (No. 188) was adopted as the initial model to refine the diffraction data of  $\text{Ba}_9\text{Co}_3\text{Se}_{15}$ . By using GSAS software packages, the refinements were conducted and smoothly converged to  $\chi^2 = 3.16$ ,  $R_p = 3.24\%$ ,  $R_{wp} = 4.61\%$ . The obtained crystallographic data and some selected interatomic distances are summarized in Table 1.

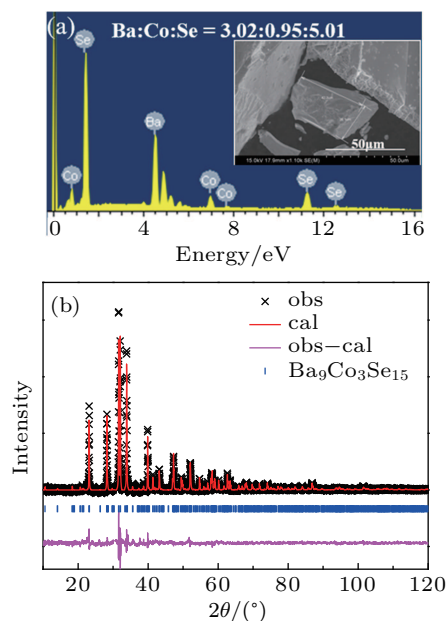


**Fig. 1.** (a) Energy dispersive x-ray spectrum collected on  $\text{Ba}_9\text{Co}_3\text{Se}_{15}$  polycrystalline samples. (b) Powder XRD patterns of  $\text{Ba}_9\text{Co}_3\text{Se}_{15}$  measured at 300 K and the refinement with the space group of  $P-6c2$  (No. 188).

**Table 1.** Crystallographic data of  $\text{Ba}_9\text{Co}_3\text{Se}_{15}$  and some selected interatomic distances in  $\text{Ba}_9\text{Co}_3\text{Se}_{15}$ .

Compound		$\text{Ba}_9\text{Co}_3\text{Se}_{15}$				
Space group: $P-6c2$ (No. 188), hexagonal						
$a = b = 9.6765(2) \text{ \AA}$ , $c = 18.9562(6) \text{ \AA}$						
$V = 1546.16(5) \text{ \AA}^3$ , $Z = 2$						
$\chi^2 = 3.16$ , $R_p = 3.24\%$ , $R_{wp} = 4.61\%$						
Atom	Label	Wyck	$x/a$	$y/b$	$z/c$	SOF
Ba	Ba1	12l	0.00688	0.36705	0.08638	1
Ba	Ba2	6k	0.38548	0.38687	1/4	1
Co	Co1	2a	0	0	0	1
Co	Co2	4g	0	0	0.16095	1
Se	Se1	12l	0.24526	0.25423	0.08187	1
Se	Se2	6k	-0.01531	0.20961	1/4	1
Se	Se3	2c	1/3	2/3	0	1
Se	Se4	4h	1/3	2/3	0.18645	1
Se	Se5	4i	2/3	1/3	0.16786	1
Se	Se6	4i	2/3	1/3	0.04253	0.5
Selected interatomic distances in $\text{Ba}_9\text{Co}_3\text{Se}_{15}/\text{\AA}$						
Co1-Co2		3.051	Co2-Co2		3.376	
Se3-Se4		3.534	Se4-Se4		2.409	
Se5-Se6		2.376	Se5-Se5		3.114	

Figure 2(a) presents the sketch of the crystal structure of  $\text{Ba}_9\text{Co}_3\text{Se}_{15}$ . The structure consists of infinite face-sharing octahedral  $\text{CoSe}_6$  chains along  $c$  axis, and these chains are triangularly arranged in the  $ab$ -plane and separated by Ba and Se atoms, demonstrating the 1D structural character. The  $\text{CoSe}_6$  chains are trimerized, leading to two sites of Co(1) and Co(2), as shown in Fig. 2(b). The distances between adjacent Co atoms in chains  $d_{\text{in-chain}}$  are 3.051  $\text{\AA}$  and 3.376  $\text{\AA}$ , respectively, while the distance between nearest neighbor Co atoms in the  $ab$ -plane  $d_{\text{in-plane}}$  is given by the lattice constant  $a = 9.6765 \text{ \AA}$ , significantly larger than  $d_{\text{in-chain}}$ . We can compare the values of  $d_{\text{in-chain}}$  and  $d_{\text{in-plane}}$  with those

of CsCoBr<sub>3</sub>, which has a similar chain structure with the infinite face-sharing octahedral CoBr<sub>6</sub> chains separated by Cs<sup>+</sup> ions. For CsCoBr<sub>3</sub>, the in-chain distance  $d_{\text{in-chain}}$  is 3.162 Å, which is very close to that in Ba<sub>9</sub>Co<sub>3</sub>Se<sub>15</sub>, while the in-plane distance  $d_{\text{in-plane}} = 7.529$  Å is much smaller than the value in Ba<sub>9</sub>Co<sub>3</sub>Se<sub>15</sub>.<sup>[18]</sup> It was reported that the intra-chain coupling strength ( $\sim 6.7$  meV) is more than fifteen times larger than the inter-chain exchange interaction ( $\sim 0.4$  meV) in CsCoBr<sub>3</sub>.<sup>[6]</sup> Thus, compared with CsCoBr<sub>3</sub>, the significantly larger  $d_{\text{in-plane}}$  in Ba<sub>9</sub>Co<sub>3</sub>Se<sub>15</sub> suggests an even weaker inter-chain coupling strength and makes Ba<sub>9</sub>Co<sub>3</sub>Se<sub>15</sub> further approach to the nature of 1D spin chain in the view of crystal structure. Besides the CoSe<sub>6</sub> chains, there exist Se-chains at the center of the triangular lattice, where the Se atoms occupy the Se(3)–Se(4) and Se(5)–Se(6) sites, respectively, as shown in Fig. 2(c). The distances of the adjacent Se atoms in the Se-chains range from 2.376 Å to 3.534 Å. The small distances of 2.376 Å and 2.409 Å are very close to the Se–Se bond length, which implies the formation of Se<sub>2</sub><sup>2-</sup> dimer in the Se-chains. The similar Se<sub>2</sub><sup>2-</sup> (Te<sub>2</sub><sup>2-</sup>) dimer has also been reported in Ba<sub>9</sub>V<sub>3</sub>Se<sub>15</sub><sup>[16]</sup> and Ba<sub>9</sub>Sn<sub>3</sub>Se<sub>15</sub> (Ba<sub>9</sub>Sn<sub>3</sub>Te<sub>15</sub>).<sup>[19]</sup>

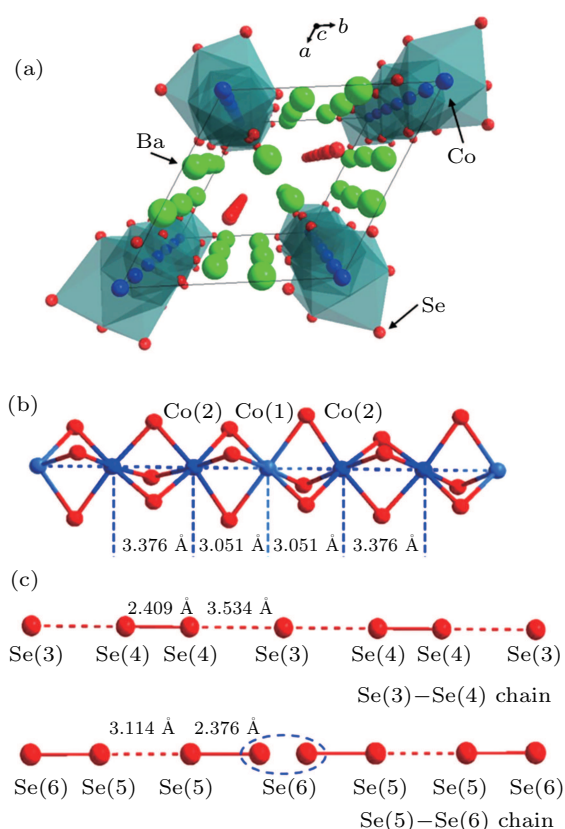


**Fig. 2.** The crystal structure of Ba<sub>9</sub>Co<sub>3</sub>Se<sub>15</sub>. (a) Top view with the projection along  $c$  axis for Ba<sub>9</sub>Co<sub>3</sub>Se<sub>15</sub>. (b) and (c) The sketch of octahedral CoSe<sub>6</sub> chains and Se chains in Ba<sub>9</sub>Co<sub>3</sub>Se<sub>15</sub>.

The temperature dependence of resistivity in Ba<sub>9</sub>Co<sub>3</sub>Se<sub>15</sub> is shown in Fig. 3(a). The resistivity increases with decreasing temperature, demonstrating a semiconducting behavior. The inset of Fig. 3(a) is the plot of  $\ln \rho$  versus  $1/T$ . The curve of

$\ln \rho(1/T)$  is a straight line in the whole measured temperature range, which indicates that the semiconducting behavior can be described based on the Arrhenius law for thermally activated conduction. By using the formula  $R \propto \exp(\Delta_g/2k_B T)$ , where  $\Delta_g$  is the semiconducting band gap and  $k_B$  is the Boltzmann's constant, the resistivity curve is well fitted and  $\Delta_g$  is calculated to be 0.748 eV, which is larger than those of Ba<sub>9</sub>Sn<sub>3</sub>Se<sub>15</sub> ( $\sim 0.5$  eV)<sup>[19]</sup> and Ba<sub>9</sub>V<sub>3</sub>Se<sub>15</sub> ( $\sim 0.2$  eV).<sup>[16]</sup>

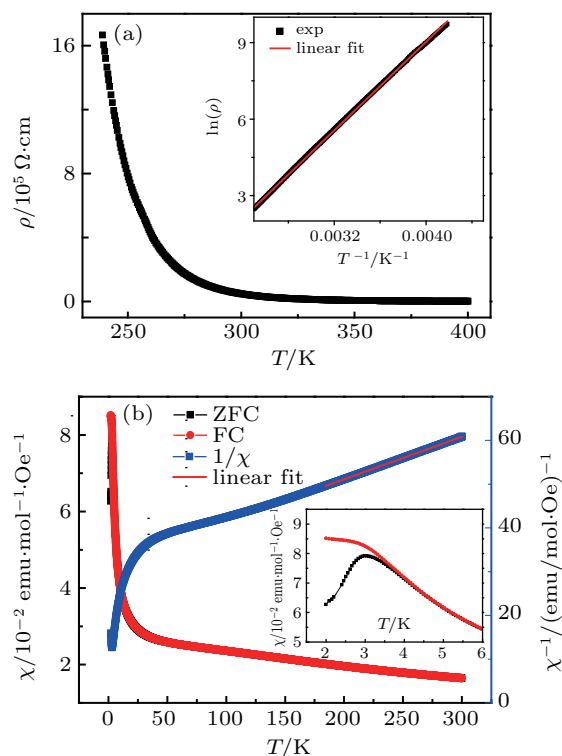


**Fig. 3.** (a) The temperature dependence of resistivity, the inset shows  $\ln \rho$  versus  $1/T$ . (b) The magnetic susceptibility  $\chi$  as a function of temperature under ZFC and FC conditions and the reverse susceptibility versus temperature. The red line is the fit of Curie–Weiss law between 200 K and 300 K. The inset shows the low temperature parts.

In order to study the magnetic properties, the dc magnetic susceptibility as a function of temperature was measured under the magnetic field of 1000 Oe in both zero-field-cooled (ZFC) and field-cooled (FC) modes, as shown in Fig. 3(b). The ZFC and FC curves are overlapped and begin to bifurcate at about 5 K, which demonstrates a  $\lambda$ -shape and suggests a spin-glass ground state with the frozen temperature about 3 K, as shown in the inset of Fig. 3(b). The inverse susceptibility versus temperature is also plotted in Fig. 3(b). In the high temperature region, the susceptibility shows a Curie–Weiss paramagnetic behavior. After fitting the susceptibility in this paramagnetic region by using the Curie–Weiss law  $\chi = C/(T - T_\theta)$ , the Weiss temperature and effective moment can be obtained to be  $T_\theta = -324$  K and  $\mu_{\text{eff}} = 5.2 \mu_B$  per Co ion, respectively. The negative sign of  $T_\theta$  indicates that the predominant interaction is antiferromagnetic. The  $\mu_{\text{eff}}$  value is typical for Co<sup>2+</sup> ( $d^7$ ,  $S = 3/2$ ), ranging from  $4.3 \mu_B$  to  $5.2 \mu_B$ .<sup>[20–23]</sup> The  $g$  factor calculated from the Curie constants ( $\mu_{\text{eff}}^2 = g^2 S(S + 1)$ ) is



2.70, and the large  $g$  factor for the  $\text{Co}^{2+}$  systems is considered to arise from the strong spin-orbital coupling and the large anisotropy.<sup>[20,21]</sup>

To verify the spin-glass feature, we carried out the ac magnetic susceptibility measurement. The temperature dependence of the real part of the ac susceptibility  $\chi'$  is shown in Fig. 4(a). Four frequencies, ranging from 133 Hz to 6373 Hz, are used to study the dynamic response of the macroscopic susceptibility. All the ac susceptibility  $\chi'$  curves display a peak at the frozen temperature  $T_f$ , with the shape similar to that of the ZFC curve of the dc susceptibility. The maximum value of  $\chi'$  decreases as the frequency increases. In addition, the frozen temperature  $T_f$  is sensitive to the frequency, which increases from 3.5 K to 4 K when the frequency increases from 133 Hz to 6373 Hz, confirming the spin-glass ground state of  $\text{Ba}_9\text{Co}_3\text{Se}_{15}$ . To characterize the spin glass, the response of susceptibility on the frequency can be quantified by the coefficient  $K = \Delta T_f / (T_f \Delta \log f)$ , as shown in Fig. 4(b). Here, for  $\text{Ba}_9\text{Co}_3\text{Se}_{15}$ ,  $K = 1.6 \times 10^{-2}$  lies in the range of  $5 \times 10^{-3} - 8 \times 10^{-2}$  for a typical spin glass system.<sup>[24]</sup>

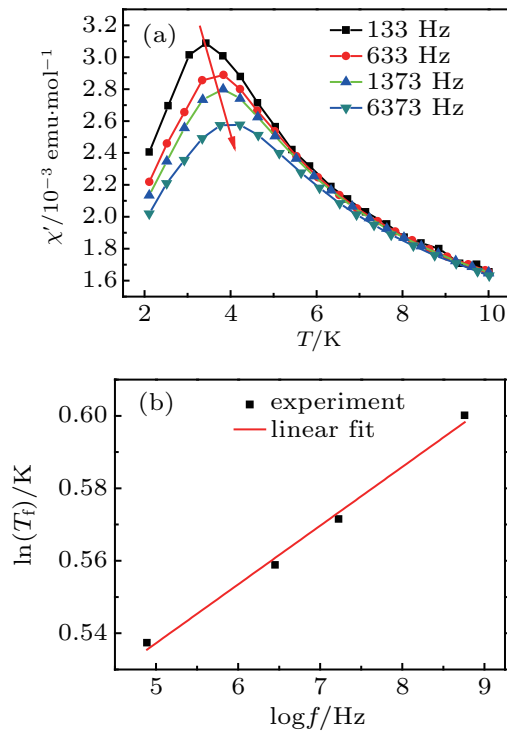


**Fig. 4.** (a) The temperature dependence real part of ac magnetic susceptibility ( $\chi'$ ) at different frequencies. (b)  $\ln T_f$  vs.  $\log f$  plot for  $\text{Ba}_9\text{Co}_3\text{Se}_{15}$ .

$\text{Ba}_9\text{Co}_3\text{Se}_{15}$  possesses a strong quasi 1D spin chain characteristic and a triangular arrangement tending to induce geometric magnetic frustration. The octahedral  $\text{CoSe}_6$  chains are arranged in a triangular lattice in the  $ab$ -plane with a significantly large distance, demonstrating a 1D chain structure. Generally, there are two energy scales for a quasi 1D spin chain system, one is the intra-chain spin coupling strength

$J_{\text{intra}}$  associated with the Weiss temperature, and the other is the inter-chain spin exchange interaction strength  $J_{\text{inter}}$ , which is usually much weaker than the intra-chain coupling and related with the temperature of long-range order formation. Using the Weiss temperature  $T_\theta$  obtained from the magnetic susceptibility measurement, we can estimate the value of  $J_{\text{intra}}$  to be about 69 K via the equation  $kT_\theta = \frac{2z}{3}S(S+1)J$ , where  $z = 2$  is the number of neighbor magnetic ions in the spin chain and  $S = 3/2$  is the spin moment. The frozen temperature  $T_f$  in  $\text{Ba}_9\text{Co}_3\text{Se}_{15}$  with a spin-glass ground state is comparable with the ferromagnetic transition temperature of 2.5 K observed in the isostructural  $\text{Ba}_9\text{V}_3\text{Se}_{15}$ , which hints that the inter-chain exchange interaction  $J_{\text{inter}}$  is very weak. Magnetic frustration usually happens in the system with the antiferromagnetic coupled spins on the triangular lattice, kagomé lattice, and pyrochlore lattice.<sup>[25]</sup> To partially release the magnetic frustration of a triangular lattice, the spins on the triangular lattice can form  $120^\circ$  angles with nearest neighbors for Heisenberg triangular antiferromagnets, and the spins can be partially ordered or fully ordered with up-up-down arrangement for Ising triangular antiferromagnets.<sup>[2]</sup> While for the other triangular-lattice compounds of candidate of spin-liquid state, such as  $\text{YbZnGaO}_4$ <sup>[26]</sup> and  $\kappa\text{-(BEDT-TTF)}_2\text{Cu}_2(\text{CN})_3$ ,<sup>[27]</sup> the spin-glass ground state was recently confirmed for the former and considered to be driven by the magnetic frustration and disorder, for the latter, no long-range order has been observed down to 75 mK and the magnetic frustration was suggested to lead to a spin-liquid state. Here, the observed spin glass behavior in  $\text{Ba}_9\text{Co}_3\text{Se}_{15}$  is speculated to mainly arise from the geometric magnetic frustration.

#### 4. Conclusion and perspectives

The new quasi one-dimension spin chain compound  $\text{Ba}_9\text{Co}_3\text{Se}_{15}$  has been synthesized under high pressure and high temperature conditions. It crystallizes into a hexagonal structure with the space group of  $P-6c2$  (No. 188). The infinite face-sharing octahedral  $\text{CoSe}_6$  chains are arranged in a triangular lattice and separated by a large distance. The compound displays a semiconducting behavior with a band gap  $\sim 0.748$  eV and a spin-glass ground state with the freezing temperature  $T_f = 3$  K. The Weiss temperature is deduced to be  $-346$  K, indicating that the predominant intra-chain exchange interaction is antiferromagnetic. It is speculated that the spin glass behavior in  $\text{Ba}_9\text{Co}_3\text{Se}_{15}$  mainly arises from the magnetic frustration due to the geometrically frustrated triangular lattice.

#### References

- [1] Mermin N D and Wagner H 1966 *Phys. Rev. Lett.* **17** 1133
- [2] Collins M F and Petrenko O A 1997 *Can. J. Phys.* **75** 605

- [3] Boucher J P, Regnault L P, Rossat-Mignod J, Henry Y, Bouillot J and Stirling W G 1985 *Phys. Rev. B* **31** 3015
- [4] Caciuffo R, Paolasini L, Sollier A, Ghigna P, Pavarini E, van den Brink J and Altarelli M 2002 *Phys. Rev. B* **65** 174425
- [5] Goff J P, Tennant D A and Nagler S E 1995 *Phys. Rev. B* **52** 15992
- [6] Mao M, Gaulin B D, Rogge R B and Tun Z 2002 *Phys. Rev. B* **66** 184432
- [7] Morishita K, Kato T, Iio K, Mitsui T, Nasui M, Tojo T and Atake T 2000 *Ferroelectrics* **238** 105
- [8] Nishiwaki Y, Tokunaga M, Nakamura T, Todoroki N and Kato T 2010 *J. Phys. Soc. Jpn.* **79** 084707
- [9] Tennant D A, Perring T G, Cowley R A and Nagler S E 1993 *Phys. Rev. Lett.* **70** 4003
- [10] Yelon W B, Cox D E and Eibschütz M 1975 *Phys. Rev. B* **12** 5007
- [11] Fagot S, Foury-Leylekian P, Ravy S, Pouget J P and Berger H 2003 *Phys. Rev. Lett.* **90** 196401
- [12] Gardner R A, Vlasse M and Wold A 1969 *Acta Cryst.* **25** 781
- [13] Imai H, Wada H and Shiga M 1996 *J. Phys. Soc. Jpn.* **65** 3460
- [14] Nakamura H, Yamasaki T, Giri S, Imai H, Shiga M, Kojima K, Nishi M, Kakurai K and Metoki N 2000 *J. Phys. Soc. Jpn.* **69** 2763
- [15] Ana Akrap, Vladan Stevanović Mirta Herak, Marko Miljak, Barišić N, Berger H and Forró L 2008 *Phys. Rev. B* **78** 235111
- [16] Zhang J, Liu M, Wang X, Zhao K, Duan L, Li W, Zhao J, Cao L, Dai G, Deng Z, Feng S, Zhang S, Liu Q, Yang Y F and Jin C 2018 *J. Phys.: Condens. Matter* **30** 214001
- [17] Larson A C and Dreele R B V 1994 *Los Alamos Natl. Lab. Rep.* **86** 748
- [18] Nagler S E, Buyers W J L, Armstrong R L and Briat B 1983 *Phys. Rev. B* **27** 1784
- [19] Zhang J, Su R, Wang X, Li W, Zhao J, Deng Z, Zhang S, Feng S, Liu Q, Zhao H, Guan P and Jin C 2017 *Inorg. Chem. Front.* **4** 1337
- [20] Hellwege K -H and Hellwege A M 1966 *Landolt-Börnstein New Series*, Vol. II/2
- [21] Yang T, Zhang Y, Yang S H, Li G B, Xiong M, Liao F H and Lin J H 2008 *Inorg. Chem.* **47** 2562
- [22] Mandrus D, Sarrao J L, Chakoumakos B C, FernandezBaca J A, Nagler S E and Sales B C 1997 *J. Appl. Phys.* **81** 4620
- [23] Barnes A D J, Baikie T, Hardy V, Lepetit M B, Maignan A, Young N A and Francesconi M G 2006 *J. Mate. Chem.* **16** 3489
- [24] Binder K and Young A P 1986 *Rev. Mod. Phys.* **58** 801
- [25] Balents L 2010 *Nature* **464** 199
- [26] Ma Z, Wang J H, Dong Z Y, Zhang J, Li S C, Zheng S H, Yu Y J, Wang W, Che L Q, Ran K J, Bao S, Cai Z W, Cermak P, Schneidewind A, Yano S, Gardner J S, Lu X, Yu S L, Liu J M, Li S Y, Li J X and Wen J S 2018 *Phys. Rev. Lett.* **120** 087201
- [27] Yamashita S, Nakazawa Y, Oguni M, Oshima Y, Nojiri H, Shimizu Y, Miyagawa K and Kanoda K 2008 *Nat. Phys.* **4** 459